Vibrational Sum-Frequency Spectroscopy of Alkane/Water Interfaces: Experiment and Theoretical Simulation

Mac G. Brown, Dave S. Walker, Elizabeth A. Raymond, and Geraldine L. Richmond*

Department of Chemistry, University of Oregon, Eugene, Oregon 97403

Received: August 9, 2002; In Final Form: October 19, 2002

The vibrational spectra of interfacial water at a series of alkane/water interfaces have been measured using vibrational sum-frequency spectroscopy. The OH stretching modes of water have been used to characterize the water−water and alkane−water interactions present at these hydrophobic/aqueous interfaces; these results are then compared with previous studies of the CCl_4/H_2O interface. The results for all alkanes examined are similar and have general spectral characteristics that coincide with the CCl_4/H_2O interface. All spectra show weaker hydrogen bonding interactions than have been observed for the vapor/water interface. Molecular dynamics calculations are used to complement the experimental results in obtaining a more complete picture of the interfacial interactions.

Introduction

In recent years, there has been a surge of theoretical and experimental interest in the determination of the structure and dynamics of water adjacent to hydrophobic surfaces.[1−8] From a theoretical standpoint, there is interest in understanding the scaling of the hydrophobic effect to large planar hydrophobic surfaces. There is also considerable interest in this topic because of its relevance to understanding a wide range of physical, biological and chemical phenomena that occur at aqueous/hydrophobic interfaces. [9,10]

Alkane/water interfaces are considered a prototypical system for studying the interaction of water with nonpolar liquid surfaces. They have also been used as model systems for the study of such biological phenomena as membrane dynamics and drug adsorption. Although there has been considerable theoretical work on alkane/water interfaces and water at other hydrophobic surfaces, comparison of this work with experimental results has been hampered by the lack of techniques that can probe this interface on a molecular level. This situation has only recently begun to change with the application of several new experimental methods that can examine liquid/liquid interfaces on a molecular level.[5−8]

In this study, vibrational sum-frequency spectroscopy (VSFS) and molecular dynamics calculations have been employed to examine in detail the structure and dynamics of the hydrogen-bonding network of water at the hexane/water, heptane/water, and octane/water interfaces. The complementary nature of the experiments and theory allows a more detailed understanding of the interface to be developed. The calculations complement the experimental studies by providing information about interfacial water molecules that are isotropically oriented and consequently not measurable by VSF. The direct and iterative comparison of the experiment with the theory also allows the testing and improvement of models used to describe water−water and water−solute interactions at these interfaces.

The results of these alkane/water studies are compared with recent experimental results of the CCl_4/H_2O interface,[6,7] where a detailed understanding of the hydrogen bonding has been obtained through a series of VSF studies including isotopic dilution experiments. Several properties of the alkane/water and CCl_4/water interfaces suggest that their molecular interfacial properties should show similar characteristics. The measured interfacial tensions of the systems are comparable, 49.7 mN/m for hexane/water and 45 mN/m for CCl_4/water.[11,12] The molecular dipole polarizabilites of hexane and CCl_4 are nearly identical,[13] 11.9×10^{-24} and 11.2×10^{-24} cm^3, respectively, also suggesting similar intermolecular interactions. Infrared experiments by Conrad and Strauss,[14,15] however, show that water dissolved in an alkane solvent rotates freely while water dissolved in CCl_4 is relatively constrained. The details of the intermolecular interactions that give rise to these macroscopic and microscopic observations dominate interfacial structure and dynamics.

Experimental Section

Vibrational sum-frequency generation is a second-order nonlinear spectroscopic technique useful for studying molecular interactions at buried surfaces.[16] This technique is sensitive to the vibrations of molecules oriented by interfacial forces, and therefore allows examination of surface molecules without overwhelming signal from the randomly oriented bulk liquids. The vibrational frequencies of water are particularly sensitive to the individual molecular environment,[17−19] allowing vibrational sum-frequency experiments to probe the interfacial hydrogen bonding network.

In a typical VSFS experiment, two sources of radiation, tunable infrared light (ω_{IR}) and a fixed frequency visible laser (ω_{VIS}), are overlapped in time and space at the interface of interest. The sum-frequency light is emitted from the interface at the sum of these two frequencies ($\omega_{SF} = \omega_{IR} + \omega_{VIS}$). When the infrared light is tuned over an interfacial vibrational mode, the quantity of sum-frequency light generated increases dramatically, creating a vibrational spectrum of the surface molecules. The sum-frequency intensity I_{SF} is given by

$$I_{SF} \alpha |\Sigma\chi^{(2)}_{R,\nu} + \chi^{(2)}_{NR}|^2 I_{VIS} I_{IR} \quad (1)$$

where $\chi^{(2)}_{R,\nu}$ is the resonant nonlinear susceptibility of vibrational mode ν, $\chi^{(2)}_{NR}$ is the nonresonant surface susceptibility, and I_{VIS} and I_{IR} are the intensities of the input laser fields. In these experiments, ssp polarization conditions are maintained for the

10.1021/jp0218589 CCC: $25.00 © 2003 American Chemical Society
Published on Web 12/07/2002

sum-frequency, visible, and infrared radiation fields, respectively. Under these polarization conditions, vibrations with dipole moment changes perpendicular to the interface are measured.

The routine used to fit the experimental spectra in this work was first developed by Bain for use in sum-frequency spectroscopy,[20] and has been used in other recent studies from this laboratory.[6,7,18,19,21] The resonant susceptibility $\chi^{(2)}_{R,\nu}$ convolves the homogeneous line width of the transition with the inhomogeneous broadening arising from the multitude of environments present in the condensed phase. Thus, each resonant peak is represented by eq 2.

$$\chi_\nu^{(2)} = \int_{-\infty}^{\infty} \frac{\mathbf{A}_\nu e^{-[(\omega_L - \omega_\nu)/\Gamma_\nu]^2}}{\omega - \omega_L - i\Gamma_L} d\omega_L \qquad (2)$$

where $\mathbf{A}_\nu$ is the complex sum-frequency transition strength. In addition to having an amplitude and a phase, each resonant peak has a center frequency (ω_ν), a homogeneous line width (HWHM, Γ_L), and an inhomogeneous line width (FWHM, $\sqrt{2 \ln 2}\Gamma_\nu$). The alkane/water spectra presented here are each fit with three resonant peaks, and zero nonresonant response. As with the CCl_4/H_2O experiments, a nonresonant sum-frequency response was not detected for these alkane/H_2O interfaces. The phases of the resonant peaks were constrained to be either 0° or 180°, with the phase of the free OH peak set to 0° as the reference point. The homogeneous line widths are fixed at 5 cm^{-1}, and it was found, as in previous CCl_4/H_2O studies,[6,18,19] that the overall spectral shape was only weakly dependent on Γ_L.

The experiments presented here were performed on a nanosecond VSF system. The details of this system have been discussed in previous publications,[6,7] so only a brief description will be given here. An Nd:YAG laser (3.5 ns pulse length, 500 mJ, 20 Hz repetition rate) is used to pump an OPO/OPA system, generating infrared light tunable from 2500 to 4000 cm^{-1}. A portion of the Nd:YAG pulse is doubled in frequency to 532 nm and brought to the interface as ω_{VIS}. The sum-frequency light generated is detected using a photomultiplier tube and boxcar integration.

The infrared and visible beams were sent to the interface through the oil phase. Scans were started at 3300 cm^{-1} to minimize heating of the interface due to absorption of the infrared light by the alkane C−H vibrations in the 2900 cm^{-1} region. Interfaces were prepared by placing ~15 mL of water in the cell followed by ~10 mL of alkane. Adding water into the cell through a syringe reduced the thickness of the oil layer to ~0.15 mm. The cell was then sealed using an IR grade silica prism, through which the visible and infrared light were brought to the interface. The visible light was kept at the critical angle for total internal reflection to maximize the sum-frequency response. The tunable infrared light (ω_{IR}) was gently focused (1 mm^2) onto the interface. The generated sum-frequency light was reflected through the prism to the photomultiplier tube, as depicted in Figure 1.

The sample cell used to contain the interfaces is constructed of Kel-F to minimize contamination of the interface. We have found that Kel-F is easier than Teflon to clean to the restrictive levels required by these experiments. Improvements in this cell and associated optics have allowed a more accurate measurement of the intensity of contributing OH modes relative to previous studies. The water used in these experiments is HPLC grade and used as delivered. The alkanes used were HPLC grade (Aldrich) and were distilled twice before use.

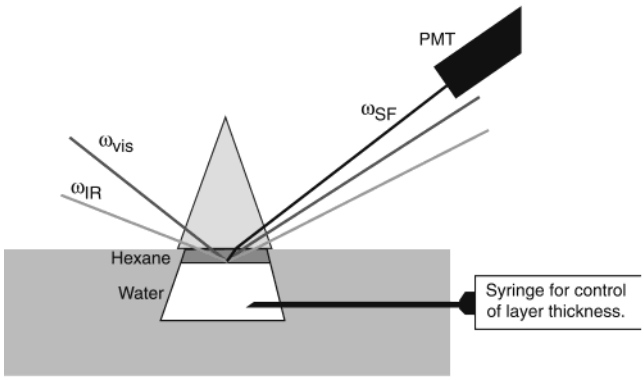

Figure 1. Schematic of the experimental cell and optical geometry. The two lasers are coupled into the alkane/water interface through an IR grade silica prism, with the sum-frequency light collected using a photomultiplier tube (PMT).

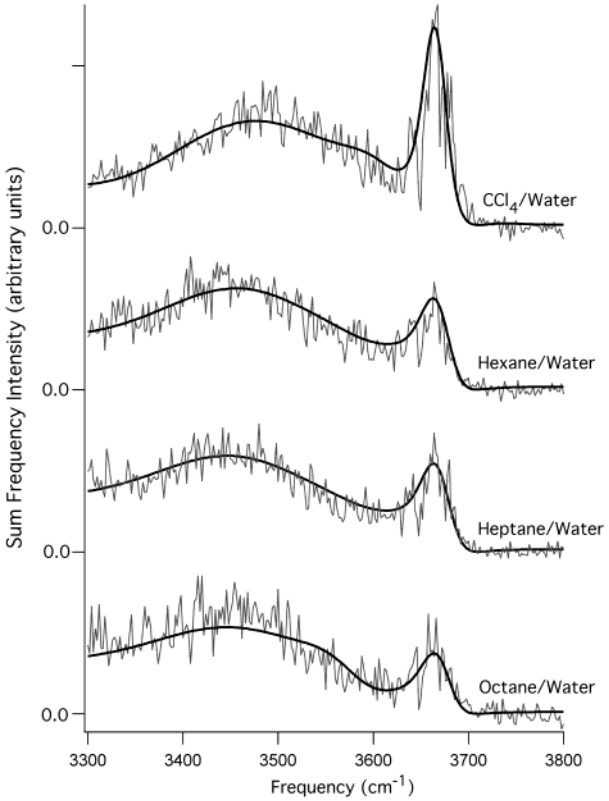

Figure 2. VSF spectra of the CCl_4/water, hexane/water, heptane/water, and octane/water interfaces. The solid lines are fits to the experimental spectra.

Experimental Results

VSF spectra of the hexane/water, heptane/water, and octane/water interfaces are shown in Figure 2 for ssp polarization, which monitors vibrational modes that have components perpendicular to the interface. The spectral region shown corresponds to the OH stretching region of water. For comparison, a spectrum of the CCl_4/water interface is also shown.[6,7] The spectra of the three alkane interfaces are very similar, suggesting that the hydrogen bonding environments of water molecules present at the hexane/water, heptane/water, and octane/water interfaces are also similar. Consequently, the general features of the spectra may be discussed together. Two obvious features are apparent in each spectrum, the most distinct being a sharp peak at 3674 cm^{-1} assigned to the uncoupled free OH. This vibrational mode occurs when an interfacial water

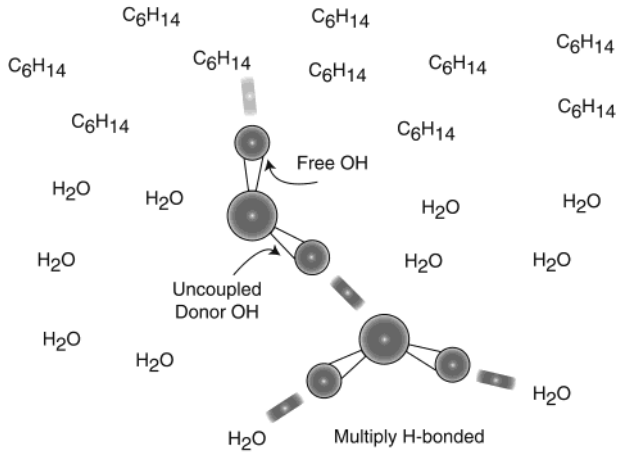

Figure 3. Schematic of the hexane/water interface.

molecule has an unbonded hydrogen directed into the oil phase while the other hydrogen protrudes into the aqueous phase. The OH stretch of the hydrogen-bonded oscillator pointed into the aqueous phase is referred to as the uncoupled donor OH. The broad feature centered at ~3450 cm^{-1} is attributed to water molecules whose OH bonds participate in hydrogen bonding with adjacent water molecules. These hydrogen-bonded vibrations include both the uncoupled donor OH bond and the vibrations of water molecules with both hydrogens involved in hydrogen bonding with other water molecules.

Using the spectral fitting procedure applied in similar previous studies,[6,7,18,19] a fit to the alkane/water data is obtained that is comprised of three peaks. The solid line represents the best fit to the data. Figure 3 is a depiction of the hexane/water interface showing water molecules in the hydrogen bonding environments represented by the assigned peaks. The VSF spectra of water at these nonpolar interfaces are dominated by the OH stretches of molecules with at least one hydrogen not participating in hydrogen bonding: the free OH mode observed at 3674 cm^{-1} and the donor OH mode observed at 3439 cm^{-1}. In contrast, the spectra of charged surfaces, such as the CaF_2/water[21] and surfactant monolayers at the air/water and CCl_4/water interfaces,[22,23] are composed primarily of the cooperative vibrations of tetrahedrally coordinated water and are observed at ~3100−3200 cm^{-1}.

Although the alkane/water and CCl_4/water spectra show similar general features, there are also notable differences in the free OH spectral feature. The free OH vibrational frequency, a sensitive probe of oil−water interactions, is shifted five wavenumbers higher in energy than the free OH vibration observed for the CCl_4/water interface at 3669 cm^{-1}. The uncertainty in peak position for the fits discussed here is approximately ±3 cm^{-1}. For comparison, the free OH peak at the vapor/water interface is measured at 3706 cm^{-1}.[19,24] Additionally, the integrated intensity of the free OH vibration relative to the donor OH vibration is smaller for the hexane/water interface than for the CCl_4/water interface. Because donor and free OH populations are required to be equal at a given interface, this difference in relative intensities between the halogenated and alkane/water interfaces must be either due to differences in the molecular orientation of these bonds, or differences in either the free or donor OH frequency distribution. MD simulation results discussed later in this paper shed insight into this issue.

The second feature observed in the spectra is a broad hydrogen-bonded peak maximized at ~3490 cm^{-1} for the CCl_4/water interface and at ~3450 cm^{-1} for the alkane/water interfaces (Figure 2). Despite the differences in location of the peak spectral intensity between the CCl_4/water and alkane/water spectra, the fits show that the uncoupled donor OH peak (3439 cm^{-1}) and the peak corresponding to the tetrahedrally coordinated water molecule vibrations (3247 cm^{-1}) are located at similar frequencies for these two types of interfaces (as shown in Table 1). The subtle difference in the shape of the spectra in the 3600−3700 cm^{-1} region for these two types of interfaces is due the absence of the weaker hydrogen bonded species found in the CCl_4/water spectrum: water molecules with both hydrogens free, either as unbonded water monomers or as hydrogen bond acceptors. The symmetric and asymmetric stretches of these water molecules are present in the VSF spectra of the CCl_4/water interface,[6,7] but do not appear to be present at a high enough concentration to be observed at the alkane/water interface. We conclude that our ability to observe them in the CCl_4/water system and not in the alkane/water systems is due to a stronger CCl_4-H_2O interaction, which orients these isolated molecules allowing them to be observed in the spectra.

TABLE 1

spectral assignment of interfacial water vibrational modes	peak frequency (ω_v/cm^{-1}) CCl_4/water[a]	peak frequency (ω_v/cm^{-1}) alkane/water
tetrahedrally coordinated	3247	3247
uncoupled donor OH	3439	3439
uncoupled Free OH	3669	3674

[a] Taken from ref 7.

It is interesting to compare these results with the studies of Conrad and Strauss for water monomers in CCl_4 and various alkanes.[14,15] In those studies the IR spectra show that the intensity of the OH stretching modes of water monomers in alkanes is significantly weaker and spreads out over a larger frequency range than that observed for monomeric water in CCl_4. In addition, water in CCl_4 exhibited a red shift in the two stretching vibrations relative to water monomers in the hydrocarbons examined, similar to what we observe for the free OH mode for the alkanes and CCl_4. It was subsequently established that monomeric water performs large angular variations between collisions with solvent molecules in the alkane systems and that water and CCl_4 form a very weak complex, thus restricting its motion.[15] Later studies of the relative degree of interaction between water and other solvent molecules indicate that water in liquid CCl_4 can be classified as intermediate between the weakly interacting water−xenon and water−alkane systems, and the stronger interacting water−benzene system.[25−29] In the water−xenon and water−alkane systems, the water rotational motion is termed "quasi-free". Although the free OH mode of the water molecules examined at these interfaces is not as free to rotate as water monomers in a bulk organic solvent, the VSF spectral observations are consistent with the monomer studies and may be suggestive of a difference in rotational freedom for water at these interfaces. Future exploration with other systems will be informative in determining how the VSF spectral features can help deduce the degree of interaction between interfacial water and the solvent, and thereby characterize the relative rotational freedom of these interfacial water molecules.

MD Simulations. Molecular dynamics (MD) simulations were performed on model hexane/water and CCl_4/water interfaces, utilizing the AMBER suite of MD programs. Molecular dynamics simulations have been shown to give accurate descriptions of the orientations and interactions of molecules at surfaces: the structure and dynamics that give rise to sum-frequency spectra.[30,31] For each system a VSF spectrum was

TABLE 2: Potential Parameters

site	q	σ(Å)	ϵ (kcal/mol)
C (CCl_4)[a]	−0.1616	3.410	0.100
Cl (CCl_4)[a]	+0.0404	3.450	0.285
O(SPC/E)[b]	−0.8476	3.166	0.155
H(SPC/E)[b]	+0.4238	0.000	0.000
C (methyl)[c]	−0.63	3.400	0.1094
C (methylene)[c]	−0.42	3.400	0.1094
H (hexane)	+0.21	2.650	0.0157

[a] Taken from Schweighofer, Essmann, and Berkowitz, ref 32. [b] Taken from ref 33. [c] Calculated from ab initio calculations as described in the text. Intramolecular parameters from AMBER.

calculated according to the method of Morita and Hynes[30,31] to allow for a direct comparison of experiment and theory.

Molecular dynamics simulations are naturally limited by the accuracy of the potential parameters used, particularly when examining the intermolecular interactions present at interfaces. Potential models were therefore chosen that have been used in previous and varied simulations.[32,33] A summary of the parameters is given in Table 2. Hexane molecules were described using the AMBER potential model that includes Lennard-Jones and Coulombic intermolecular interactions, as well as the SHAKE algorithm. The AMBER parm94 data set was used to parametrize these intra- and intermolecular interactions. An ab initio calculation was performed on an all-trans *n*-hexane molecule using SPARTAN 5.1 to obtain appropriate atomic charges for use in the simulation. The Hartree−Fock calculation was run at the 6-31G* level, and charges were placed on the atoms according to the natural charge distribution available in the Spartan package. The results of the calculation are given in Table 2.

The CCl_4 potential was taken from simulations by Schweighofer et al.[32] on the interactions of sodium dodecyl sulfate at the CCl_4/water interface. An ab initio calculation was performed on CCl_4, using the same methods as described for hexane to check for consistency in the atomic charges used between the hexane and CCl_4 potential models. Near perfect agreement was found between the calculation and the charges proposed by Schweighofer.[32]

The SPC/E potential model[33] was used to describe the water molecules in these simulations and the interactions between different molecular species were performed using the standard Lorentz−Berthelot combination rules. The SPC/E and CCl_4 potential models are based on rigid molecule point charge and Lennard-Jones interactive forces and are easily implemented within AMBER.

A snapshot of the simulated hexane/water interface is shown in Figure 4a. The CCl_4/water simulation was designed in a similar fashion. A rectangular simulation cell (24.939 Å × 24.939 Å × 74.817 Å) containing hexane and water molecules was used to create the two interfaces approximately 25 Å apart. Equilibration was performed for each liquid separately before creation of the simulation cell.

Initially, 511 water molecules were placed randomly in a (24.939 Å)^3 box. The system was run through 2000 energy minimization steps to remove any unfavorable contacts between molecules. The water was then equilibrated at 1300 K for 100 ps followed by further equilibration at 300 K for 100 ps, both under constant volume conditions. Temperature control was maintained through the Berendsen thermostat with 0.2 ps coupling.[33] The total energy and temperature were followed throughout the equilibration process. The system was considered equilibrated when the total energy and temperature remained constant for at least 50 ps.

A similar process was used to create an equilibrated (24.939 Å)^3 cell of hexane molecules. The number of hexane molecules was chosen to reproduce the experimental density. After equilibrating the two fluids separately, the hexane simulation cell was duplicated and the resulting three boxes were placed together with periodic boundary conditions to generate two interfaces, as shown in Figure 4a. The energy of the system was minimized until convergence to relieve any unfavorable molecular contacts created by joining the simulation boxes. The overall system was then equilibrated at 300 K and constant volume conditions for 200 ps. This methodology was found to consistently arrive at an equilibrated interfacial system. Identical procedures were followed for calculations on the CCl_4/water interface.

Molecular coordinates for statistical analysis and spectral generations were collected for 200 ps following equilibration. These equilibrated runs were performed at 300 K rather than room temperature to account for any heating of the experimental system by the lasers used. Coordinates were sampled every 50 time steps (every 0.05 ps). Artificial smoothing of the interfaces was avoided by using the center of mass of the bulk water as the system origin in all system analysis.

Computational Modeling of a Sum-Frequency Spectrum. A brief description of the techniques used to generate a VSF spectrum from the MD simulation data is given here. For more details, the reader is referred to the excellent paper by Morita and Hynes on the air/water interface.[30] Creation of the VSF spectra from the molecular coordinates available from MD simulations requires the calculation of a vibrational frequency and the contribution to the total interfacial nonlinear susceptibility ($\chi^{(2)}$) for each OH bond in the system.

The SPC/E potential is a rigid body description of a water molecule, making the direct calculation of vibrational frequencies impossible. The vibrational frequency of each OH bond is therefore determined from the tension in the OH bond arising from the interaction with its nearest neighbor. The linear dependence of the OH bond tension on the vibrational frequency given by Morita and Hynes was assumed.[30] This treatment of bond tension predicted a vibrational frequency of ∼3333 cm^{-1} for a typical OH stretch participating in a hydrogen bond as compared to the 3439 cm^{-1} observed experimentally. In all cases, the bond tension was scaled by 80% before calculating vibrational frequencies to give better agreement with experiment. If no neighboring water oxygen was found within 2.5 Å, the OH bond was considered a free OH oscillator and no interaction with water was calculated. Instead, the interaction with the hexane or CCl_4 molecule that gave rise to the largest tension in the OH bond was used to determine the vibrational frequency.

In deriving an interfacial VSF spectrum, the sum-frequency response ($\chi^{(2)}_{ssp}$ amplitude) of each hydrogen-bonded species must be calculated, not just the number density of each species. To determine $\chi^{(2)}_{ssp}$, the contribution of the molecular hyperpolarizability β of each OH bond to the total interfacial nonlinear susceptibility under ssp polarization conditions is found using the Euler angle transformation matrix,

$$\chi^{(2)}_{ssp} = \Sigma_{ijk}\mu_{ssp:ijk}:\beta_{ijk} \quad (3)$$

where i, j, and k are the molecular frame axes and the values of β_{ijk} are taken from the calculations of Morita and Hynes. The transformation matrix $\boldsymbol{\mu}$ applies the Euler angles to transform the β_{ijk} elements from the molecular frame into the laboratory frame, as defined by the polarizations of the incident light.[34] In general, the more perpendicular an OH bond is to the interface, the greater its ssp sum-frequency response. A net orientation

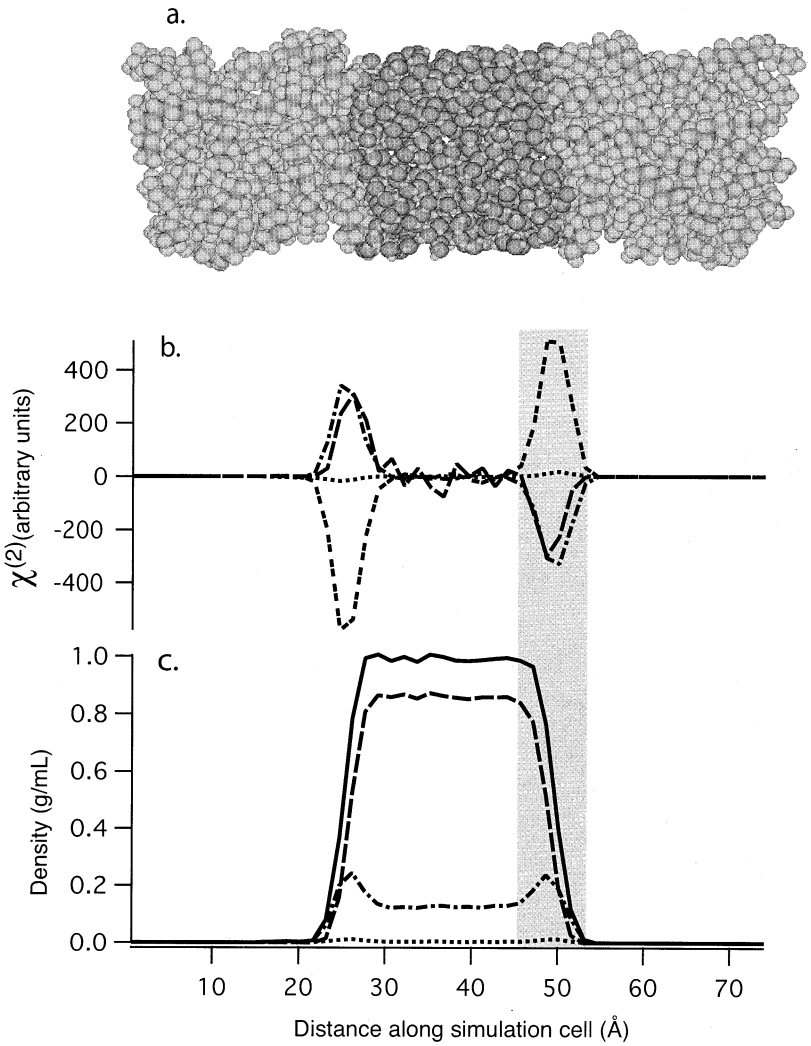

Figure 4. (a) Snapshot of the simulation cell for hexane/water. (b) Nonlinear susceptibility determined from the MD simulations. The contributing species are the free OH (- - -), donor OH (-·-), water molecules with both hydrogens bonded (— —) and those with neither hydrogen bonded (· ·). (c): Density histogram for water and the contributing species from (b). The line symbols are the same as they are in 4b. The solid line is the total density. Donor OH and free OH contributions are equal.

of molecules is required for sum-frequency generation, and the depth of this orientation determines the surface sensitivity of VSF spectroscopy. Random distributions of molecules have no net contribution to SF spectra.

The nonlinear susceptibility $\chi^{(2)}_{ssp}$ can be calculated for each interfacial species as a function of distance along the simulation cell to determine how each species contributes to the sum-frequency signal, and to what depth sum-frequency is generated. This representation is however only a first approximation of the sum-frequency probe depth, as the frequency dependence has not yet been included. It is the most relevant measure of interfacial thickness for sum-frequency experiments, however, as it indicates to what distance the water molecules are influenced by the presence of the interface.

A direct comparison of experimental and simulated results requires that the contribution of each OH bond to the total $\chi^{(2)}_{ssp}$ amplitude be multiplied by a factor, linear in frequency, which accounts for the greater infrared vibrational response for modes at lower frequency.[30] This enhancement factor can be quite large for typical OH frequency shifts. A vibration at 3400 cm^{-1}, for example, has an enhancement factor of ~3.5 relative to an unperturbed OH stretch, resulting in an enhancement of ~12 when the intensity ($|\chi^{(2)}_{ssp}|^2$) is calculated. The contribution of each OH vibration to the total VSF spectrum is therefore dependent on both the individual vibrational frequencies and the molecular orientation.

Coupling the vibrations, once the frequency and the value of $\chi^{(2)}_{ssp}$ for both OH vibrations are known, involves a relatively simple 2 × 2 matrix diagonalization. A coupling constant of 49.5 cm^{-1} is assumed, giving rise to the experimentally observed symmetric and antisymmetric vibrations of gas phase water (3756 and 3657 cm^{-1}). The eigenvalues and eigenvectors of the resulting matrix are used to arrive at two new, coupled frequencies and $\chi^{(2)}_{ssp}$ amplitudes for the water molecule in its individual molecular environment. No intermolecular coupling of OH vibrations is included in these simulations.

The final step in the process is to place these molecular vibrations into the spectrum. Two unsquared Lorentzians, representing the two vibrations of each water molecule, are assigned the resonant vibrational frequencies and $\chi^{(2)}_{ssp}$ amplitudes determined above. Each vibration is then separated into real and imaginary components. A line width of 22 cm^{-1} is assumed in order to maintain consistency with the work of Morita and Hynes.[30] This is done for each molecule in the system, and for each time step to generate a statistically averaged vibrational sum-frequency spectrum. By separately adding the real and imaginary components of each vibration before squaring, interferences between different molecular vibrations

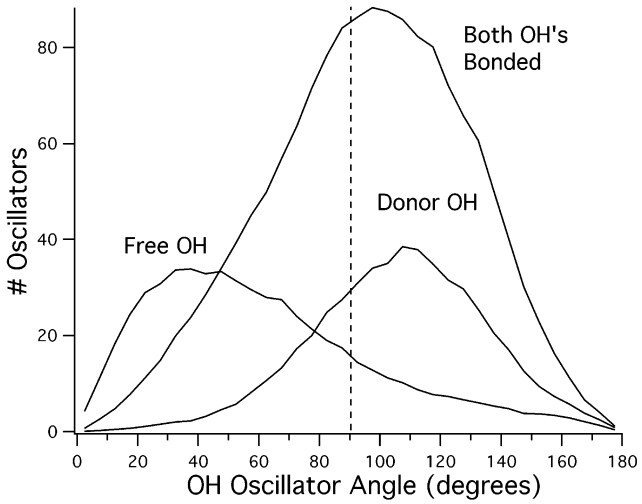

Figure 5. Orientational distributions for OH oscillators relative to the interface (represented by a dotted line at 90°). 0° points along the surface normal into the hexane. The direction of the permanent dipole moment was used to determine the angle for those water molecules with both OH oscillators bonded. Distributions represent a 1.5 Å slice at ~26 Å.

are allowed. The squares of the total real and imaginary spectral components at each frequency are then added to generate a VSF spectrum.

Computational Results

Monitoring the influence of hydrogen bonds on particular interfacial water molecules allows different hydrogen bonding environments to be identified. Figure 4b shows a plot of $\chi^{(2)}_{ssp}$ amplitudes for OH bonds in these different hydrogen bonding environments along the length of the hexane/water simulation cell. The two interfaces in the simulation cell are mirror images of each other, and so give rise to opposite signs of $\chi^{(2)}_{ssp}$. In the center of the cell water molecules experience no orienting interfacial forces and so the individual contributions to $\chi^{(2)}_{ssp}$ cancel to zero. On the right side of the box, the plot of $\chi^{(2)}_{ssp}$ shows a large positive susceptibility for the free OH oscillators, and two smaller negative peaks for the donor and multiply hydrogen-bonded species. The signs and amplitudes of these peaks can be understood by examining the orientational distributions shown in Figure 5. On average, the free OH is oriented out of the interface (~30° from normal) with very little cancellation, so a large sum-frequency response is expected. The donor OH bonds however are oriented roughly parallel to the interface, pointing only slightly into the bulk water phase (~110° from normal), resulting in a significantly smaller and oppositely signed contribution to $\chi^{(2)}_{ssp}$ than free OH bonds. No correction for $\sin(\theta)$ sampling was made; the distributions shown represent the actual populations of water molecules within the simulation. Although the number of donor and free OH bonds is the same, the susceptibility arising from the donor OH is considerably smaller; this is attributed to the largely in-plane nature of the donor OH bonds. The interfacial forces also orient water molecules with both hydrogen atoms participating in hydrogen bonding. These molecules are found, on average, to have both of their hydrogens near the plane of the interface but pointing slightly toward the bulk water (~95° from normal). A small contribution to $\chi^{(2)}_{ssp}$, opposite in sign from the free OH signal, is observed from these water molecules. Contributions to $\chi^{(2)}_{ssp}$ from polarizability within the plane of the interface, though significant, largely cancel due to the isotropic nature found within the interfacial plane. These angular distributions used to calculate $\chi^{(2)}_{ssp}$ correspond well with previous simulations of hydrophobic interfaces.[30,35−39]

Figure 4c shows the relative density of several water species at the hexane-water interface, in addition to the total calculated water density. The largest fraction of water molecules have both hydrogens participating in hydrogen bonding. As the number of free and donor OH oscillators are required to be the same, the density histograms for the two species are identical; however, an increased number of free and donor OH oscillators is seen at the interface, which is expected. A small contribution is observed by water molecules with both hydrogens free but their density is extremely low relative to the other types of water species.

The interfacial depth probed by VSF experiments can be estimated from the simulation results by examining the $\chi^{(2)}_{ssp}$ amplitude and density plots in Figure 4. The simulated hexane/water interface, for example, displays a net orientation of water molecules for a total of 9 Å, as evidenced by the nonzero value of $\chi^{(2)}_{ssp}$ on each side of the box. The full width at half-maximum of the surface $\chi^{(2)}_{ssp}$, an alternative estimate of interfacial depth, is ~4.5 Å. Results for the CCl_4/water interface are similar. While the majority of the sum-frequency signal arises from the traditionally defined interfacial region (95%−5% water density), orientational order (i.e. nonzero susceptibility) persists ~3 Å into a region occupied entirely by water molecules. Previous simulations,[39] as well as X-ray scattering experiments on alkane/water interfaces,[8] have suggested that the hexane/water and CCl_4/water interfaces are molecularly sharp, with interfacial widths due to surface roughness or capillary waves rather than a diffuse mixing region. These simulations support the conclusion that the interfaces are not a diffuse mixed region, but also show that orientational order persists into the bulk density region.

The VSF spectra calculated from these MD simulations for the hexane/water and the CCl_4/water interfaces are shown in Figure 6. A comparison of the simulated results with the experimental spectra of Figure 2 shows excellent general agreement. In both cases, a sharp free OH peak is observed at ~3700 cm^{-1} as well as a broad feature centered at ~3400 cm^{-1} arising from both the donor OH and molecules participating in two and more hydrogen bonds. The relative intensities of the vibrational features are comparable to experiment for both the CCl_4/water and hexane/water interfaces. Certain differences are evident. The simulated free OH frequencies are higher than experimentally observed, indicating that the average oil−water interaction energy experienced in the simulation is too weak. This is perhaps not surprising, as the parameters that define the potential energy between disparate molecular species are rarely experimentally constrained. Further refinement of the simulation and analysis, through the use of more sophisticated polarizable potential models and through the inclusion of more than nearest neighbor molecules in the force calculation, should allow for a more accurate determination of the frequency of oscillation of weakly interacting water molecules. The symmetric and asymmetric stretches of nonbonded water are not observed in the simulation, suggesting that the creation of these molecules is a rare event, not observed on the time scale of the simulation. Molecular dynamics simulations are limited by computer speed, making it difficult to study through simulation the creation of uncommon species such as nonbonded water molecules.

The relative reduction in free OH intensity for the hexane/water interface as compared to the CCl_4/water interface is observed in the simulated spectra, allowing a direct comparison of experiment and theory. An analysis of the orientations of

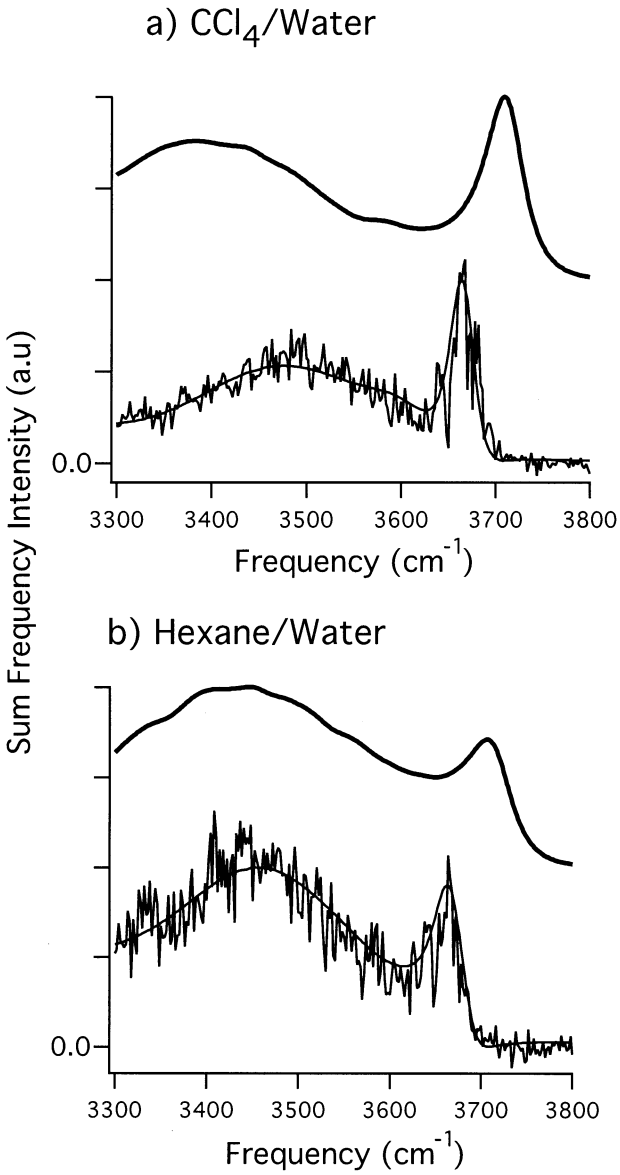

Figure 6. Calculated (offset) and experimental sum-frequency spectra for the CCl_4/water and hexane/water interfaces.

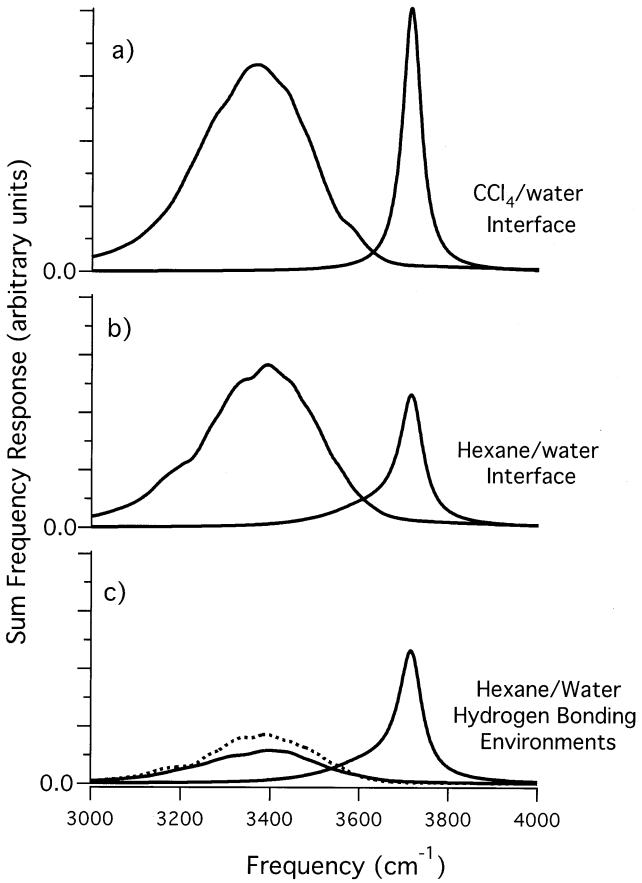

Figure 7. Calculated components contributing to the theoretical spectra of the CCl_4/water (a) and hexane water (b) interfaces, respectively. (c) Contributing factors for the broad, redshifted peak in the hexane/water interface are separated into donor OH (solid) and tetrahedrally bonded (dashed) components.

OH bonds in different hydrogen bonding environments, a possible explanation for the variation in observed free OH intensities, however, shows no obvious differences between the two interfaces. The orientational distribution of water molecules shown in Figure 5 for the hexane/water interface is essentially identical to those observed for the CCl_4/water interface (not shown). Another comparison of water orientation can be made by adding up the frequency independent $\chi^{(2)}_{ssp}$ amplitudes along the simulation cell, as shown in Figure 4b for the hexane/water interface. No clear differences between the hexane/water and CCl_4/water interfaces are evident, indicating that the VSF spectral differences between the two simulated interfaces are not due to the orientational distributions of water in these systems.

The simulated spectra of the hexane/water and CCl_4/water interfaces have been broken down into separate free OH and hydrogen bonded OH vibrations in Figure 7 to allow a further comparison of the two interfaces. The free OH vibration of the CCl_4/water interface (Figure 7a) is a symmetric peak centered at $\sim$3700 cm^{-1}, indicative of weak interactions between the CCl_4 and water. The free OH for the hexane/water simulations, however, is asymmetric, with significant intensity observed from 3600 to 3700 cm^{-1} (Figure 7b). The integrated intensity of the free OH vibrational components is similar between the two interfaces, suggesting that the number density of the free OH oscillators is the same. Although the sharp peak at $\sim$3700 cm^{-1} suggests that the majority of the hexane−water interactions are weak, the asymmetry to lower energy suggests that some stronger hexane-water interactions are present that are not seen in the CCl_4/water simulations. This suggests that the shift of a portion of the free OH intensity to lower frequencies is responsible for the reduction in peak free OH intensity for the simulated hexane/water interface. This lower frequency intensity overlaps with the hydrogen-bonded region of the spectrum, and creates asymmetrical spectral features that are difficult to include in experimental fits.

The hexane/water simulation has been further broken down into separate free OH, uncoupled donor OH and tetrahedrally coordinated vibrations in Figure 7c. No collective vibrations of tetrahedrally coordinated water molecules (experimentally observed at $\sim$3250 cm^{-1} and lower[40]) are expected in the simulation because the intermolecular coupling of OH vibrations is not included in this treatment. Because only nearest neighbor interactions were considered, the peak frequency corresponding to tetrahedrally coordinated water molecules (dashed) is significantly blueshifted, almost directly on top of the peak corresponding to the donor OH vibration (solid). The peak frequency of the donor OH vibration is at $\sim$3410 cm^{-1}, rather than the 3439 cm^{-1} experimentally observed. These limitations suggest that further refinement of the calculations of simulated

frequency shifts is necessary, to create better agreement between experiment and theory.

Summary and Conclusions

The VSF spectra of the three different alkane/water interfaces have been examined and compared with previous studies of the CCl_4/water interface.[6,7] All of these systems show similar general molecular characteristics. For all interfaces examined, the hydrogen bonding exhibited between water molecules (as probed perpendicular to the interface) is dominated by those that have less than tetrahedral coordination. In fact the two primary peaks observed in all systems correspond to water molecules that hydrogen bond to two or fewer water molecules. In contrast, the spectra of polar surfaces, such as the CaF_2/water [21] and surfactants at air/water interfaces,[23] show the distinctive signature of cooperative vibrations of tetrahedrally coordinated water. The vapor/water interface also displays a higher proportion of strongly hydrogen-bonded water molecules.[19,41,42] The frequency of the free OH vibration is found to be slightly lower for CCl_4/H_2O, which we conclude to be due to an average water−CCl_4 interaction at the interface that is weak but stronger than the average alkane−water interfacial interactions. The intensity of the free OH peak for the alkane/water systems is also smaller than what is found for CCl_4/H_2O, which is consistent with a weaker average water−alkane interaction that could lead to less constrained rotational motion of interfacial water molecules. The hydrogen-bonded region for the two types of interfaces are very similar with the predominant intensity observed at $\sim$3460 cm^{-1}.

Molecular dynamics calculations on these interfaces give rise to simulated spectra that reproduce the experimental results, including the differences in free OH intensity. No intermolecular cooperativity is built into the model calculations, but the agreement between the experimental and simulation spectra further supports the observation that the vibrations in the VSF spectrum arise mostly from water molecules with little cooperative motion. There is a relatively large density of molecules at the interface that have both hydrogens bonded to other water molecules but due to the largely in-plane orientation of their dipoles and their isotropic orientation with regards to the surface normal, a relatively small VSF signal is observed from these molecules under ssp polarization. The orientations observed for water molecules are consistent with previous calculations, as well as with fits to the experimentally observed spectra.

Interestingly, the simulations suggest that a small fraction of the free OH oscillators at the surface interact fairly strongly with hexane. These interactions, which pull the free OH vibration to slightly lower frequency, contribute to the observed difference in free OH intensity between alkane/water and CCl_4/water systems. Recent studies by Scheiner and Kar discuss the existence of CH−O complexes that exhibit properties similar to those observed in weak hydrogen bonding systems.[43] Further VSF investigation into other systems will provide more information on the details of these oil−water interactions. The agreement of experiment and theory observed for these systems suggests that our understanding of the spectroscopy of nonpolar interfaces is converging.

Acknowledgment. The authors are grateful for the funding provided for this work from the National Science Foundation (CHE-9725751) for the experimental studies and the Office of Naval Research for the initiation of the MD simulation studies. DSW is grateful for the support of a Department of Energy GAANN Fellowship (#P200A010820).

References and Notes

(1) Lum, K.; Chandler, D.; Weeks, J. D. *J. Phys. Chem. B* **1999**, *103*, 4570−4577.
(2) Huang, D. M.; Chandler, D. *J. Phys. Chem. B* **2002**, *106*, 2047−2053.
(3) Stillinger, F. H. *J. Solution Chem.* **1973**, *2*, 141−158.
(4) Tanford, C. *The Hydrophobic Effect: Formation of Micelles and Biological Membranes*; Wiley-Interscience Publications: New York, 1973.
(5) Du, Q.; Freysz, E.; Shen, Y. R. *Science* **1994**, *264*, 826−828.
(6) Scatena, L. F.; Richmond, G. L. *Science* **2001**, *292*, 908−911.
(7) Scatena, L. F.; Richmond, G. L. *J. Phys. Chem. B* **2001**, *105*, 11240−11250.
(8) Mitrinovic, D. M.; Zhang, Z.; Williams, S. M.; Huang, Z.; Schlossman, J. L. *J. Phys. Chem. B* **1999**, *103*, 1779−1782.
(9) Chipot, C.; Wilson, M. A.; Pohorille, A. *J. Phys. Chem. B* **1997**, 782−791.
(10) Pohorille, A.; Wilson, M. A. *J. Chem. Phys.* **1996**, *104*, 3760−3773.
(11) Bartell, D. J. D. a. F. E. *J. Phys. Chem.* **1952**, *52*, 480−484.
(12) Girifalco, L. A.; Good, R. J. *J. Phys. Chem.* **1957**, *61*, 904−909.
(13) *CRC Handbook of Chemistry and Physics*, 73rd ed.; Boca Raton, FL, 1993.
(14) Conrad, M. P.; Strauss, H. L. *Biophys. J.* **1985**, *48*, 117−124.
(15) Conrad, M. P.; Strauss, H. L. *J. Phys. Chem.* **1987**, *91*, 1668−1673.
(16) Shen, Y. R. *Mater. Res. Soc. Symp. Proc.* **1986**.
(17) Scherer, J. R. In *Advances in Infrared and Raman Spectroscopy*; Clark, R. J. H., Hester, R. E., Eds.; Heyden: Philadelphia, 1978; Vol. 5, pp 149−216.
(18) Brown, M. G.; Raymond, E. A.; Allen, H. C.; Scatena, L. F.; Richmond, G. L. *J. Phys. Chem. A* **2000**, *104*, 10220−10226.
(19) Raymond, E. A.; Tarbuck, T.; Richmond, G. L. *J. Phys. Chem. B* **2002**, *106*, 2817−2820.
(20) Bain, C. D.; Davies, P. B.; Ong, T. H.; Ward, R. N.; Brown, M. A. *Langmuir* **1991**, *7*, 1563−1566.
(21) Becraft, K.; Richmond, G. L. *Langmuir* **2001**, *17*, 7721−7724.
(22) Gragson, D. E.; Richmond, G. L. *J. Phys. Chem. B* **1998**, *102*, 569−576.
(23) Gragson, D. E.; Richmond, G. L. *J. Am. Chem. Soc.* **1998**, *120*, 366−375.
(24) Raymond, E. A.; Tarbuck, T. L.; Brown, M. G.; Richmond, G. L. *J. Phys. Chem.* **2003**. In press.
(25) Danten, Y.; Tassaing, T.; Bresnard, M. *J. Phys. Chem. A* **2000**, *104*, 9415−9427.
(26) Zoidis, E.; Yarwood, J.; Tassaing, T.; Danten, Y.; Besnard, M. *J. Mol. Liq.* **1995**, *64*, 197−210.
(27) Klemperer, W. *Nature* **1993**, *362*, 698.
(28) Suzuki, S.; Green, P. G.; Bumgarner, R. E.; Dasgupta, S.; Goddard, W. A., III.; Blake, G. A. *Science* **1992**, *257*, 942.
(29) Besnard, M.; Danten, Y.; Tassaing, T. *J. Chem. Phys.* **2000**, *113*, 3741.
(30) Morita, A.; Hynes, J. T. *Chem. Phys.* **2000**, *258*, 371−390.
(31) Morita, A.; Hynes, J. T. *J. Phys. Chem. B* **2002**, *106*, 673.
(32) Schweighofer, K. J.; Essmann, U.; Berkowitz, M. *J. Phys. Chem. B* **1997**, *101*, 3793−3799S.
(33) Berendsen, H. J. C.; Grigera, J. R.; Straatsma, T. P. *J. Phys. Chem.* **1987**, *91*, 6269−6271.
(34) Hirose, C.; Akamatsu, N.; Domen, K. *Appl. Spectrosc.* **1992**, *46*, 1051−1072.
(35) Lee, C. Y.; McCammon, J. A.; Rossky, P. J. *J. Chem. Phys.* **1984**, *80*, 4448−4455.
(36) Buuren, A. R. v.; Marrink, S.-J.; Berendsen, H. J. C. *J. Phys. Chem.* **1993**, *97*, 9206−9212.
(37) Carpenter, I. L.; Hehre, W. J. *J. Phys. Chem.* **1990**, *94*, 531−536.
(38) Chang, T.-M.; Dang, L. X. *J. Chem. Phys.* **1996**, *104*, 6772−6783.
(39) Michael, C.; Benjamin, I. *J. Phys. Chem.* **1995**, *99*, 1530−1536.
(40) Richmond, G. L. *Annu. Rev. Phys. Chem.* **2001**, *292*, 257−285.
(41) Miranda, P. B.; Shen, Y. R. *J. Phys. Chem. B* **1999**, *103*, 3292−3307.
(42) Schnitzer, C.; Baldelli, S.; Schultz, M. J. *Int. Rev. Phys. Chem.* **2000**, *19*, 123−153.
(43) Scheiner, S.; Kar, T. *J Phys. Chem. A* **2002**, *106*, 1784−1789.